Spectroscopic investigations of atmospheric pressure microwave torch nitrogen plasma jet

V. Foltin

Dept. Exerimental Physics, Faculty of Mathematics, Physics and Informatics, Comenius University, Mlynská dolina, 84248 Bratislava, Slovakia

L. Leštinská, Z. Machala

Dept. Astronomy, Earth Physics and Meteorology, same address, e-mail: vfoltin@fmph.uniba.sk, machala@fmph.uniba.sk

Received 2 May 2006

Microwave (MW) torches are typically used to produce equilibrium plasmas for various industrial applications. We present spectroscopic investigations of atmospheric pressure afterglow plasmas generated by a Litmas Red MW torch (2.45 GHz, 3 kW) in nitrogen. We employ optical diagnostics: emission spectroscopy and digital photography to characterise the plasma jet. Contrary to standard MW torch geometries (where the gas flows upstream the cavity perpendicular to the MW wave guide), we use special nozzles where the gas is inserted via two tangential inlets on top of the MW cavity. Plasma produced into the torch swirls up tangentially through the inlet. We tested several nozzles with different gas inlet angles and diameters. We present a systematic study of the nitrogen afterglow plasma jet parameters. Varying MW power and gas flow rates results in varying plasma jet sizes and properties. The more energy is inserted in the flowing gas, the greater emission and higher plasma temperatures are obtained. Plasma temperatures are determined from the CN violet system by comparing experimental and simulated (LIFBASE) spectra. Axial profiles of the emission intensity and photo–documentation characterise the evolution of the jet in space. A small admixture of oxygen results in different excited states chemistry, which was apparent from the emission spectra.

PACS: 52.75.Hn
Key words: microwave plasma torch, atmospheric pressure afterglow plasma jet, emission spectroscopy

1 Introduction

Considerable interest exists in medium– to high–power atmospheric pressure microwave (MW) sustained plasmas for environmental and industrial processing as well as for diagnostics and monitoring applications. The main advantages of such plasmas are electrodeless operation, high–throughput atmospheric processing, efficient MW–to–plasma coupling, and availability of inexpensive sources at 0.915 and 2.45 GHz. Low power (500 W) atmospheric pressure MW–induced plasmas have had a long history of use for laboratory spectroscopic analysis instrumentation. Such plasmas can be formed in resonant cavity, waveguide, or surface–effect systems, typically in argon, helium, nitrogen, or air [1]–[4]. Recently, there have been studies and applications of higher power ($>$ 1 kW) MW plasmas to increase

plasma robustness for laboratory spectroscopic analysis [5]–[8], continuous emissions monitoring in the field [9], commercial processing [10], and other applications [11]. Atmospheric MW plasmas can operate over a wide range of electron plasma density regimes from low–density glow–discharge–like plasmas [10, 11] to higher density arc–discharge–like torch plasmas [5]–[9].

The work reported here concerns a spectroscopic study of an atmospheric pressure MW torch afterglow plasma jet in nitrogen. We investigated the emission spectra of the plasma jet, the emission intensity at various wavelengths (corresponding to specific molecular transitions) as functions of varying MW power, gas flow rates, height and in some experiments also the concentration of oxygen admixture. By comparing measured and simulated spectra we determined plasma temperatures for some specific plasma regimes. These investigations will serve as a platform for further dual–discharge experiments aimed at producing large volume non–equilibrium atmospheric plasmas required by many environmental, technical, and diagnostics applications.

2 Experimental setup

MW Plasma Torch. Litmas Red MW plasma torch powered by a 5 kW magnetron (National Electronics, NL10230–1 supplied from Richardson Electronics switching power generator SM1050) was used to generate atmospheric pressure plasma with properties close to the local thermodynamic equilibrium (LTE). The magnetron has a maximum power output of 3 kW. The torch is able to generate air plasmas in the temperature range $750 \div 4\,700$ K the gas flow rates $8 \div 110$ l/min (at normal conditions) [12, 13]. In this study we use nitrogen gas (with purity 99.99 and 99.999 %) or nitrogen with a small admixture of oxygen. The temperature and velocity of the plasma jet can be set by varying the output power and the gas flow rate. The MW torch system was externally cooled with water and air. We designed and tested a new type of nozzles: The gas is inserted tangentially downstream though the nozzle into the internally cooled cylindrical plasma cavity made of hardened Teflon placed inside the MW resonator, thus causing a swirl gas flow in the cylinder. The generated swirling plasma is consequently blown out upstream through the central orifice (10 mm) of the nozzle (contrary to the typical torch systems with upstream flows perpendicular to the microwaves [7, 8]). We tested two nozzles designed with slightly different geometries for lower and higher gas flow rates: nozzle 1 (up to 30 l/min), and nozzle 2 ($20 \div 60$ l/min). A schematic view of the experimental arrangement is shown in Fig 1. The MW discharge is ignited by pneumatic insertion of a metal ignator into the plasma cavity synchronized with microwaves from the magnetron. The brush–like ignator causes a local enhancement of the electric field resulting in discharge ignition. As soon as the discharge is ignited (in time $< 0,5$ s) the ignator returns back from the cavity.

Optical diagnostics. A light emitted from the plasma jet is collected with an aperture and then focused with a fused silica lens onto two fibre optics separated by a beam–splitter positioned at 45°. The fibre optics lead into an Ocean Op-

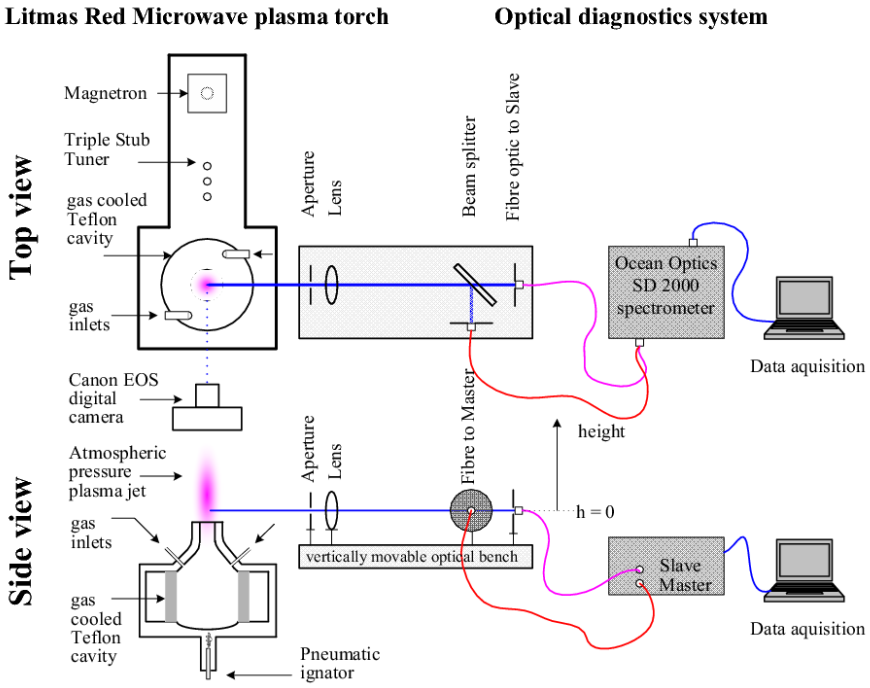

Fig. 1. Experimental setup – schematic view.

tics SD2000 dual spectrometer, fitted with two grating/CCD combinations. The two 1 200 and 600 grooves/mm gratings provide coverage of these spectral ranges: Master 200 ÷ 500 nm, and Slave 500 ÷ 1 100 nm. The optical train is mounted on a translation stage, which enables vertical movement along the nozzle axis. The plasma jet shapes were simultaneously documented with a digital camera Canon EOS 300D.

3 Results and discussion

A) Typical emission spectra for Nitrogen. In spite of using nitrogen for plasma generation, we mostly observed very strong CN molecular spectra: CN violet ($B^2\Sigma^+ - X^2\Sigma^+$) and CN red system ($A^2\Sigma - X^2\Sigma^+$), and very weak N_2 (second $C^3\Pi_u - B^3\Pi_g$ and first $B^3\Pi_g - A^3\Sigma_u^+$ positive systems), as well as N_2^+ ($B^2\Sigma_u^+ - X^2\Sigma_g^+$ first negative system) [14]. The typical CN spectra with certain vibrational transitions identified are shown in Fig. 2. This observation indicates a presence of carbon–containing impurities in the plasma that result in forming excited CN radicals. In order to identify the source of carbon we tested high purity N_2 (99.999 %). Despite one order of magnitude higher purity, the CN signal in the emission spectra dropped only to about the half of the original signal with N_2 (99.99 %). This indicates that most of carbon impurity does not come from the feeding gas but is

released from the MW cavity as the temperature increases, most likely from the rubber o–rings sealing the Teflon cylinder.

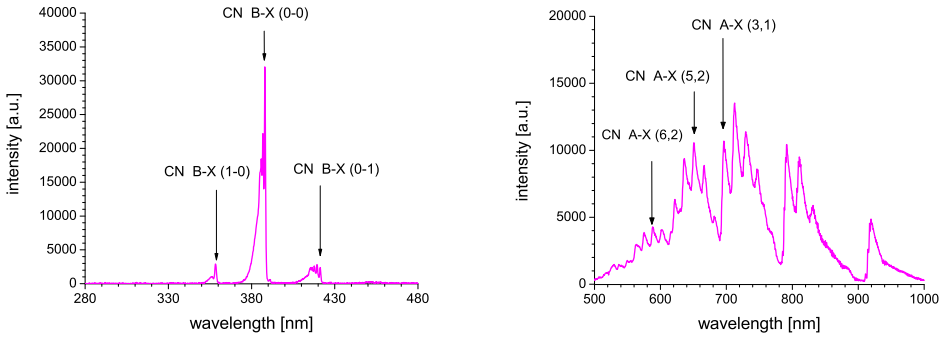

Fig. 2. Spectra of CN violet (left) and red (right) systems, Nozzle 1, $P = 1.46$ kW, $Q = 13$ l/min, $h = 0$ mm

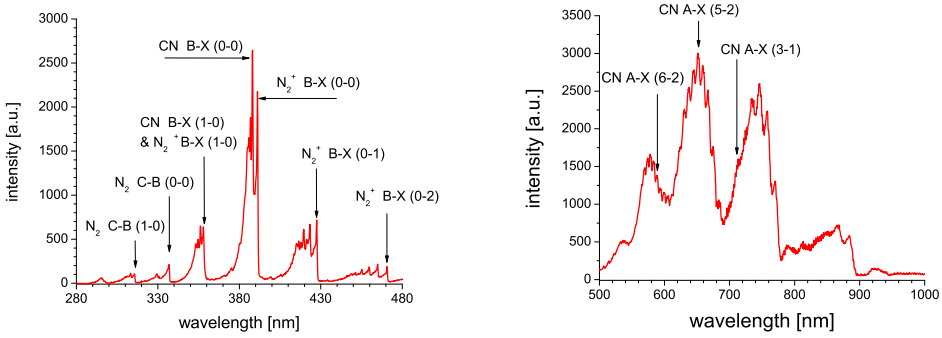

Fig. 3. Spectra of N_2, CN, N_2^+, Nozzle 2, $P = 1.46$ kW, $Q = 29$ l/min, $h = 0$ mm

This result was confirmed when we operated nozzle 2 designed for higher flow rates. In this case, the interior of the MW cavity is not heated so much and so considerably less carbon is released from the rubber o–rings. The typical spectra from the nitrogen plasma jet are shown in Fig. 3. CN spectra are still present, however, they are much less intense. On the other hand, N_2 and N_2^+ spectra become more apparent.

B) Experiments with varying MW power and energy density. MW power was varied in the range from 0.97 to 1.78 kW. The value of the power P entering the plasma is given as: $P = P_{\mathrm{mag}} - P_{\mathrm{ref}}$ with P_{mag} being the power supplied from the magnetron and P_{ref} is the reflected power. At optimal settings of tuning screws P_{ref} can be neglected, hence $P = P_{\mathrm{mag}}$. Fig. 4 shows the emission intensity at

certain wavelengths corresponding to the particular vibrational transitions in the CN violet and red systems as a function of the MW power. These measurements were carried out with a flow rate $Q = 15$ l/min and at the height $h = 0$ mm of the plasma jet, (i.e. in the axial position at the very end of the nozzle orifice). Intensity of radiation increases with increasing power at all particular wavelengths. The same effect can be observed from the photo–sequence (Fig. 6).

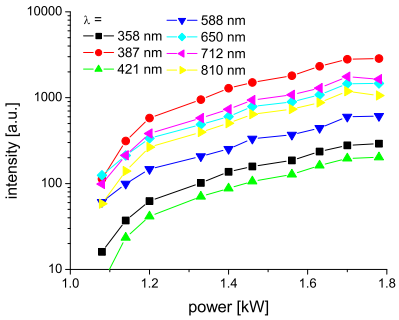

Fig. 4. Emission intensity as a function of power. Nozzle 1, $Q = 15$ l/min, $h = 0$ mm.

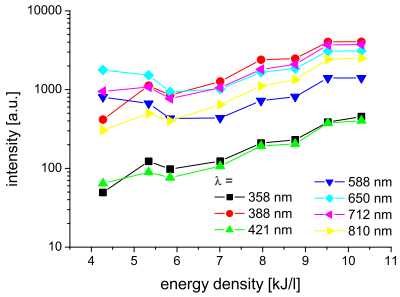

Fig. 5. Emission intensity as a function of energy density, Nozzle 1, $h = 0$ mm.

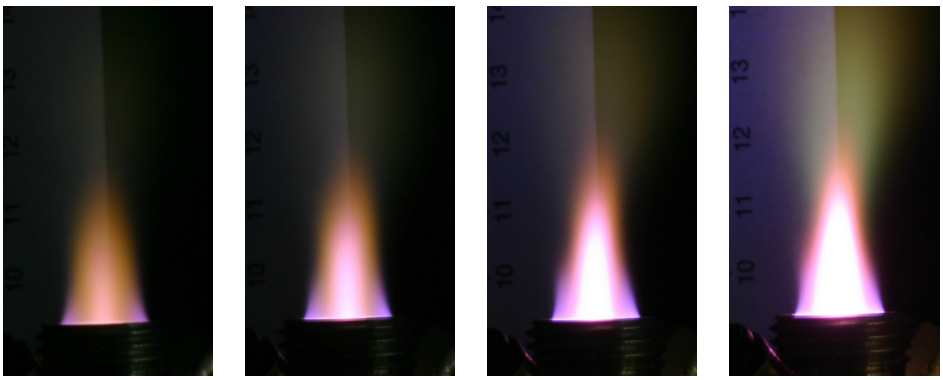

P = 0.97 kW P = 1.14 kW P = 1.46 kW P = 1.78 kW

Fig. 6. Plasma jet photographs, nozzle 1, varying P and fixed Q = 15 l/min. Exposure 2 s, aperture 22.

In order to compare experiments carried out not only with varying power P but also with varying gas flow rate Q, we integrate these two parameters in one: energy density. Energy density is defined as the energy dissipated in the volume of the treated gas [J/l] and can be calculated as $w = P/Q$. Fig. 5 shows the intensity of radiation as a function of the energy density at specific wavelengths. Intensity increases with increasing energy density.

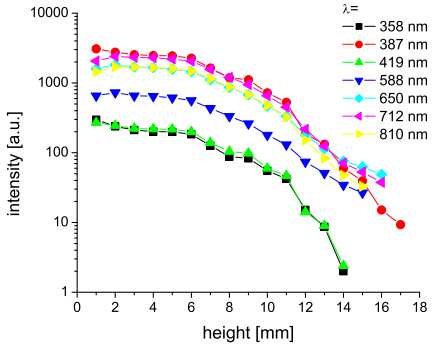

Fig. 7. Vertical profile of the emission intensity. Nozzle 1, $P = 1.46$ kW, $Q = 13$ l/min..

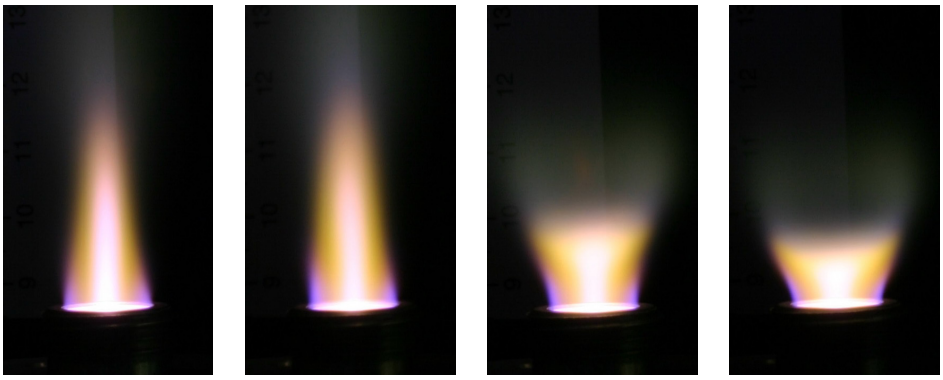

Q = 36 l/min Q = 47 l/min Q = 50 l/min Q = 60 l/min

Fig. 8. Plasma jet photographs, nozzle 2, varying Q, fixed $P = 1.78$ kW. Exposure 1 s, aperture 22.

C) Vertical profile of the plasma jet. We investigated the vertical axial profile of the emission intensity of the plasma jet in the height range from 0 to 25 mm from the orifice of the nozzle, at a fixed $Q = 13$ l/min and $P = 1.46$ kW. This profile for several specific wavelengths can be seen in Fig. 7. The emission intensity from the afterglow plasma decreases with increasing height.

D) Afterglow plasma shapes. The plasma jet shape was always conical with nozzle 1, with all powers and flow rates. With nozzle 2 designed for higher flow rates, on the contrary, at certain Q specific for every P the conical jet shape collapses into an interesting funnel–like shape (e.g. at $P = 1.78$ kW this value is about 50 l/min). This collapse is photo–documented in Fig. 8. Explaining this interesting phenomenon requires further investigations. It is most likely related with the

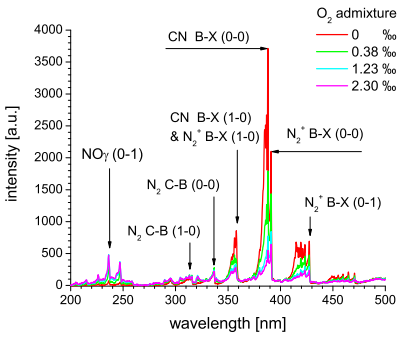

Fig. 9. Emission spectra of N_2 plasma jet (Q = 26 l/min) with various O_2 admixtures.

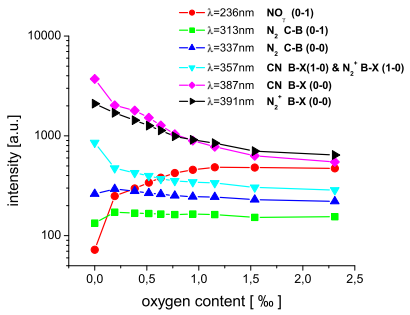

Fig. 10. Emission intensities of various excited species in N_2 plasma jet as functions of O_2 content.

complex geometrical, thermal and flow properties of the hot swirling plasma.

E) Nitrogen plasma with small oxygen admixture. In all experiments with nitrogen plasma jet we detected CN emission, as discussed previously (section A). Although CN emission was due to the presence of a minor carbon–containing impurity, it was usually very strong. On the other hand, in previous experiments carried out in air [12, 13], no CN emission was found. To verify the effect of oxygen we added a small amount of O_2 into the N_2 flow and investigated the emission spectra. Significant changes in emission spectra depending on the O_2 content were observed. With O_2 present, newly found NO ($A^2\Sigma^+$–$X^2\Pi_r$) bands appeared in $210 \div 260$ nm region and their intensity increased with O_2 content. On the contrary, with increased O_2 concentration the CN intensity decreased (Figs. 9, 10). Interestingly, the intensity of N_2^+ bands also decreased with O_2 content. An explanation of this effect requires further investigations and a detailed insight into the kinetics of plasma chemical reactions of the involved excited species.

F) Determining plasma temperatures from the emission spectra. Emission spectroscopy is a powerful tool for measuring rotational T_r and vibrational T_v plasma temperatures. At atmospheric pressure, rotational temperature equilibrates with the gas temperature ($T_\mathrm{g} \approx T_\mathrm{r}$) owing to fast collisional relaxation. T_v compared to T_r indicates whether the plasma is in the state of LTE. For determining the plasma temperatures we employed a simulation program LIFBASE [15], which calculates spectra of various species and transitions (e.g. CN violet, N_2^+ first negative) at set T_r and T_v. We then compared the simulated spectra with the measured ones and found the best fits. For illustration we present the results for two experiments in N_2 with nozzle 1:

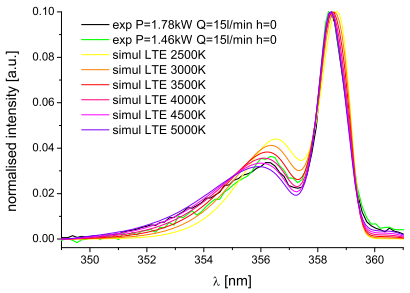

Fig. 11. Comparison of experimental and simulated CN B–X (1–0) LTE spectra.

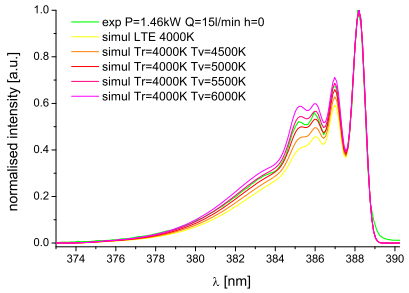

Fig. 12. Comparison of experimental and simulated CN B–X (0–0) at $T_\mathrm{r} = 4\,000$ K and various T_v.

Exp. 1: $P = 1.78$ kW, $Q = 15$ l/min, $h = 0$ mm,
Exp. 2: $P = 1.46$ kW, $Q = 15$ l/min, $h = 0$ mm.

- We first assumed the plasma in the LTE state. By comparing simulated and measured spectra for Exp. 1 and Exp. 2 we found plasma temperatures of $4\,500 \pm 500$ K and $4\,000 \pm 500$ K, respectively. Comparison of simulated and measured spectra is given in Fig. 11.
- Since the obtained LTE fit was not perfect, we suspected the plasma to be slightly non–LTE. We thus simulated spectra with $T_\mathrm{v} > T_\mathrm{r}$. One of the obtained fit is shown in Fig. 12.
  For Exp. 1: $T_\mathrm{r} = T_\mathrm{g} = 4\,500 \pm 500$ K and $T_\mathrm{v} = 5\,000 \pm 500$ K.
  For Exp. 2: $T_r = T_\mathrm{g} = 4\,000 \pm 500$ K and $T_\mathrm{v} = 5\,300 \pm 500$ K. This confirms that generated plasma is slightly non–LTE but close to the LTE state.

A more detailed temperature study of the plasma jet at various operation regimes, with temperature as a function of power, flow rate and energy density, as well as with the radial temperature profiles, will be presented in future.

4 Summary

We presented spectroscopic characterisation of atmospheric pressure afterglow plasma jet generated by a 3 kW microwave torch in nitrogen with special nozzles causing a swirl flow. Varying MW power and gas flow rates results in varying plasma jet sizes and properties. The more energy is inserted in the flowing gas, the greater emission and higher plasma temperatures are obtained. Axial vertical profiles of the emission intensity and photo–documentation characterise the evolution of the jet in space. At high gas flow rates (50 l/min), the conical shape of the jet collapses into a funnel shape. Plasma temperatures were determined by comparing experimental and simulated (LIFBASE) spectra of CN, which was found a dominant

radiative system due to carbon impurities. A small admixture of oxygen results in the decrease of CN and increase of NO and N_2 emission, which indicates different excited states chemistry. These results will serve as a platform for further experiments aimed at environmental, technical, and diagnostics applications of MW plasma jets.

This work was carried out under the support of the Slovak Grant Agency VEGA 1/2013/05 and 1/3043/06 grants and NATO EAP.RIG 981194 grant. We gratefully acknowledge Sencera, Ltd. for loaning us the MW torch. We thank professors V. Martišovitš and R. Hajossy for their valuable advice and M. Janda for LaTeX conversion.

References

[1] A. T. Zander et al.: Appl. Spectrosc. **35/4** (1981) 357.

[2] K. Fallgatter et al.: Appl. Spectrosc. **25** 3 (1971) 347.

[3] K. A. Forbes et al.: J. Anal. At. Spectrom. **6** (1991) 57.

[4] K. C. Ng and W. L. Shen, Analyt. Chem. **58** (1986) 2084.

[5] Y. Okamoto, Analyt. Sci. **7** (1991) 283.

[6] K. Ogura et al.: Appl. Spectrosc. **51**, 10 (1997) 1496.

[7] K. M. Green et al.: IEEE Trans. Plasma Sci. **29** (2001) 399.

[8] H. Matusiewicz: Spectrochim. Acta. **47B** 10 (1992)1221

[9] P. P. Woskov et al.: Waste Management **20** (2000) 395.

[10] H. Potts and J. Hugill: Plasma Sources Sci. Technol. **9** (2000) 18.

[11] J. E. Brandenburg et al.: IEEE Trans. Plasma Sci. **26** (1998) 145.

[12] Z. Machala et al.: AIAA **2003–874** (2003) 1.

[13] Z. Machala, C .O. Laux and C. H. Kruger.: *Nonequilibrium Microwave and DC Discharges in Atmospheric Pressure Air*, Gordon Research Conference on Plasma Processing Science (2002) 1.

[14] C. O. Laux: *Optical Diagnostics and Radiative Emission of Air Plasmas*, PhD thesis, Mechanical Engineering, Stanford University 1993.

[15] J. Luque and D. R. Crosley, SRI Report MP 99–009 (1999) 1.